Design and Analysis of a Myoelectric Arm Prosthesis for Transradial Amputees working as Auto-Mechanics

Azzam Afghani P. Alonto, Christian Ericson P. Delos Santos, Aaron Randall Jardenil and Alan Miguel Joaquin M. Ocho
De La Salle University Integrated School, Manila

Abstract: Amputees struggle to function because of the large degree of dependence they need to execute basic tasks that people could normally do. Amputees usually opt to use a prosthesis, for cosmetic and other functional reasons, which are not often made for situations with intense physical exertion such as the workplace. Thus, this study aims to create a mechanical arm prosthesis design that is occupationally suitable for transradial amputees. The device is mostly made of acrylonitrile butadiene styrene (ABS), a type of thermoplastic. A digital model of the prosthesis, divided into three subassemblies, was created via Autodesk Inventor. These then went through Finite Element Analysis in which a 400 N load was placed to simulate a pushing force. After the simulations, it was proven that the individual subassemblies can withstand the specified force with minimal displacement and without yielding which shows that larger forces could be exerted. This also shows that ABS is a suitable material for creating such assistive devices. Further study could be made by optimizing the geometry and changing the orientation of the loads.

Key Words: pwds; transradial amputees; prosthetics; assistive device; finite element analysis

1. INTRODUCTION

Currently, there are about 1.44 million people with disabilities (PWDs) in the Philippines (Philippine Statistics Authority, 2013). According to Mina (2013), 93 out of 123 persons with mobility impairment in urban areas are either underemployed, unemployed, or apart from the labor force. It is inferable based on this data that there is a substantial number of people with missing limbs in the Philippines, either congenitally or externally, who have a difficult time getting a steady source of income.

In specifically the case of upper limb amputees, there are different situations where a person would need to get an upper limb (arms, wrists, or hands) amputated. Indications include trauma beyond repair, irreparable loss of the blood supply of that limb, malignancy, severe contracture, infection, congenital deformities, burns, electrical injury, frostbite, and complications from diseases (Maduri & Akhondi, 2018). As for the causes of these indications, except for the disease and congenital related ones, some common examples would be machinery accidents, infrastructural accidents, as well as military and athletic injuries. For these patients to cope with daily life despite their limb loss, various types of prostheses were developed.

Transradial and Congenital Transradial Amputation both refer to the loss or the absence of the forearm or anything below it, including the wrist and the hand (Ovadia & Askari, 2015). The only difference is that the former refers to an accident or an unnatural amputation caused by outside factors, and the latter refers to a birth defect. To assist people with this condition, prostheses are developed.

A prosthesis, which is an artificial device that replaces a missing body part (Strait, 2006), was designed to solve this problem and help PWDs be more financially and physically independent. Its structural integrity was analyzed through finite element analysis. ABS or acrylonitrile butadiene styrene, a thermoplastic aliphatic polyester derived from renewable sources, was the set material for the prototype. Additionally, it utilized sensors that monitor nerve activity in muscles, known as Electromyography sensors (Vigotsky et al., 2018), to aid in its functionality. The model was constructed in Autodesk Inventor and virtually tested in Autodesk Nastran In-CAD. The prosthesis design is made for a person who is a transradial or congenital transradial amputee.

2. METHODOLOGY

2.1. Prosthesis Design

The arm prosthesis was created through Autodesk Inventor, which is a computer-aided design (CAD) software that excels in manufacturing modeling. The design process was divided into two main parts: the extension, which is the main load-bearing structure, and the terminal end, which is the

tool. The extension was primarily made of ABS and its length was based on the arm dimensions of an average Filipino man. As stated in a study by Rahmann, et al. (2018), the average forearm-to-hand length for Filipinos is 44.1cm, while the average hand length is 19.8 cm. Other dimensions such as stump length, arm diameter near the elbow, and wrist diameter were based on a sample arm with dimensions 15 cm, 9 cm, and 7 cm respectively. Though there are no maximum dimensions as to how long the stump should be, the 15 cm length was chosen as it provides enough space for the other internal components of the device without surpassing the average forearm length. The aforementioned dimensions of the prosthetic were utilized for experimentation, but the design will be made adaptable when it is set for public use. This means that the dimensions of the device, particularly the forearm length and diameters, will change to enhance the cosmetic appearance of the amputee's arm and the contact of the device to the stump. Additionally, a stretchable socket and an adjustable harness will be used to cater to the varying sizes of the arm stump and circumference. However, this was not presented in the virtual model as it is not needed in the finite element analysis. Moreover, the tool (wrench) was designed to have an effective length of 49.16 cm since it mimics the effective length of the hand combined with a model car wrench of 40 cm.

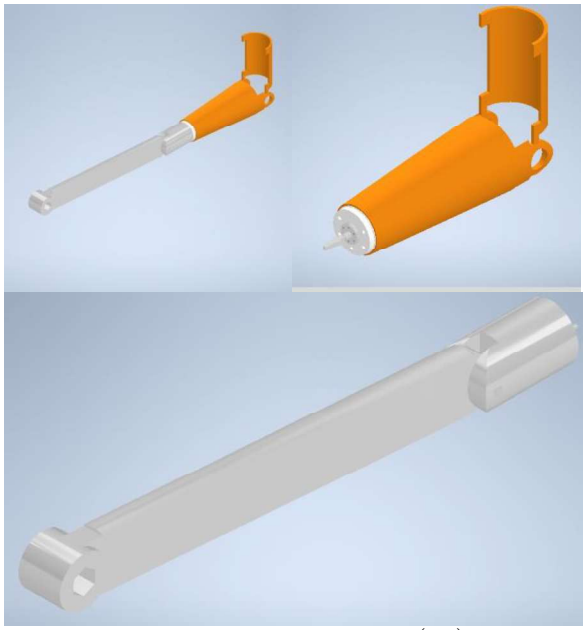

Fig 1. Full assembly of prosthetic arm (left), assembly of extension (right), assembly of sample tool (bottom)

2.2. Finite Element Analysis

The design of the prototype was only tested through virtual means with the use of Autodesk Nastran In-CAD software, which was chosen since it is directly integrated within the modeling software. The main test involved was the linear stress tests wherein the load-bearing components of the prosthesis were analyzed by subassemblies. There are three subassemblies: the exterior shell, the motor with a shaft extension, and the sample tool, which were highlighted as orange, white, and gray in Figure 1 respectively. For each subassembly, their respective constraints, connections, and areas of load application were defined. A force of 400 N was applied as a pushing force since it is the force required to produce a torque of 145 ft/lbs when using the sample tool. The chosen torque is considered to be the maximum torque required to tighten and remove a lug nut from a car tire (Tirerack, 2021). The torquing of lug nuts is a common task in auto-mechanics, specifically in vulcanizing, hence becoming the chosen force. These loads will be applied longitudinally to simulate a pushing force to determine whether the design can tolerate the applied forces. The basis of a successful model was determined on two types of analyses: (a) von Mises stress test, and (b) safety factor. All areas of the model must retain a von Mises stress value lower than the material's stress yield. Additionally, the safety factor must verify the structural integrity of the model by providing a value greater than 1. Any unsatisfied condition would indicate that the model has yielded and must undergo modifications. These parts were not tested as a full assembly due to the limitations of the software. Further characterization is applied by analyzing displacement results.

3. RESULTS AND DISCUSSION

3.1. Analysis of Exterior Shell Subassembly

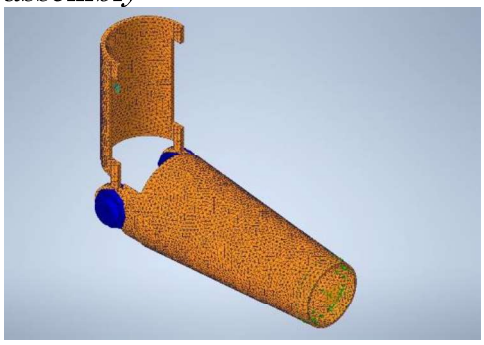

Fig 2. Specified constraints, loads, connections, and generated mesh for exterior shell subassembly

The subassembly presented in Figure 2 consists of two joined pieces wherein the vertical piece rests on the upper arm and the horizontal piece is where the stump is inserted. These two parts are joined by a bolt (presented as a blue entity in Figure 2) that is aligned with the elbow joint. The length of

the horizontal piece is 243 mm, which was achieved by obtaining the difference of the average hand-to-forearm length and average hand length as presented by Rahmann, Dawal, Yusoff, and Kamil (2018). The diameter of the hole at the rear end of the piece is 90 mm while the diameter at the front end is 70 mm. These dimensions were determined by the model arm. Additionally, the thickness of the material is consistently 5 mm thick in both components. The location and direction of the applied load are seen at the terminal end heading inward the horizontal component as represented by the green arrows in Figure 2.

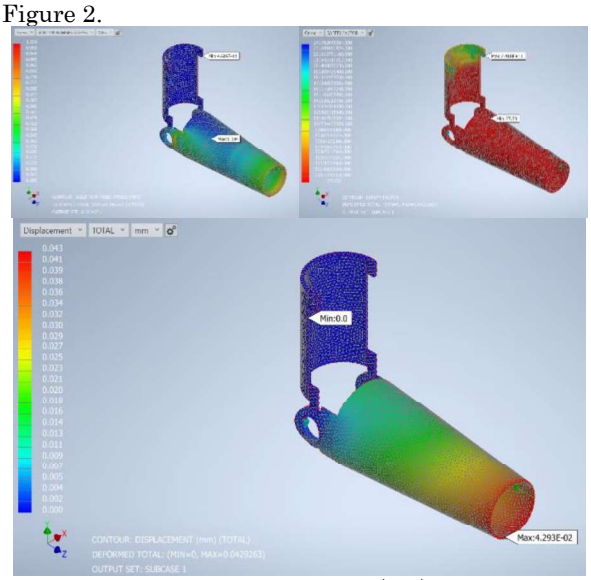

Fig 3. von Mises stress analysis (left), safety factor analysis (middle), and displacement analysis (right) of exterior shell subassembly

The material used for both components is ABS, which has a yield stress (point of shift from elastic to plastic deformation) of 20 MPa. It has a Young's modulus of 2240 and Poisson's ratio of 0.38. As seen in Figure 3, the maximum stress experienced by the model is 1.034 MPa, which is significantly lower than the yield stress. This indicates that the component would be able to withstand greater forces. Additionally, the minimum value of the safety factor analysis is far beyond 1, giving a value of 27.23. Such value would imply that the structure has no risk of yielding and is safe for use under the applied force. The displacement analysis as presented in Figure 3 shows that there is minimal deformation throughout the model. Since the maximum value, indicated by red zones in the analysis, is 0.043 mm, then it is suitable to describe that the subassembly is highly stable.

3.2. Analysis of Motor with Shaft Extension Subassembly

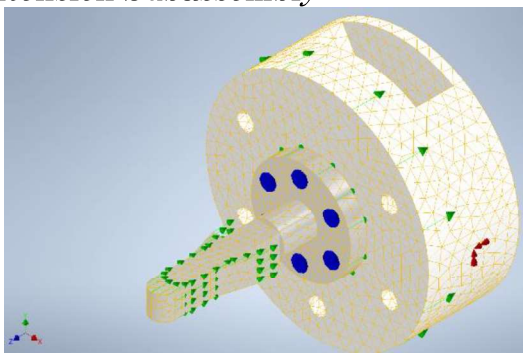

Fig 4. Specified constraints, loads, connections, and generated mesh for motor subassembly

The subassembly as presented in Figure 5 is composed of three components: (a) motor casing, (b) servo motor, and (shaft extension). The motor casing is where the servo motor fits for it to be attached to the exterior shell. Its outer surface is where the constraints are placed (as marked by the red arrows in Figure 4) due to its connection to the previous subassembly. The outer radius of the casing is 70 mm and the inner radius is 30 mm in order to fit the motor. Due to the short shaft of the motor, with a measurement of 12.4 mm, a shaft extension made of steel was added. Screws (as depicted blue in Figure 4) we used at the base of the extension to connect the extension to the shaft. Moreover, the geometry of the shaft extension is wide at half of its length so that it would serve the purpose of being part of the locking mechanism. All the components were identified to be made of steel in the finite element analysis software. The load is applied on the entire front surface as represented by the green arrows pointing towards the rear end in Figure 4.

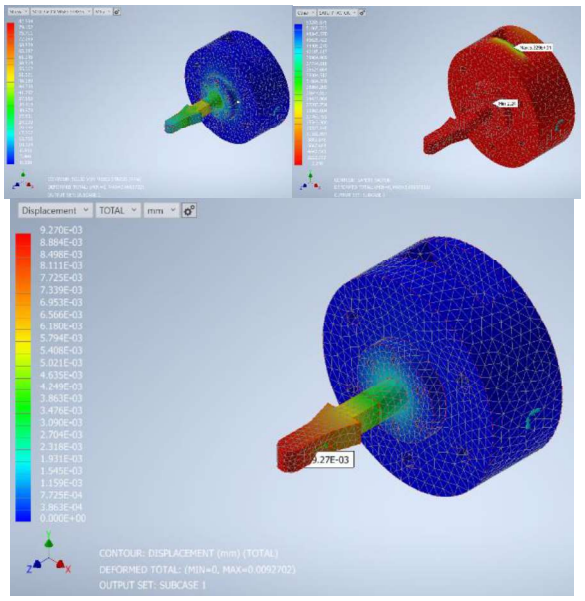

Fig 5. von Mises stress analysis (left), safety factor analysis (middle), and displacement analysis (right) of motor subassembly

With the material set to steel, its modulus of elasticity, Poisson's ratio, and yield strength are 210000, 0.3, and 207 MPa respectively. The solid von Mises stress analysis shows that the maximum stress value is 82.594 MPa, which satisfied the first condition for the success of the subassembly. It is, however, important to observe that the area with the most stress is located at the surface of the motor, which would indicate that modifications could be made to distribute the force around the casing instead of the electrical component. Nonetheless, the current state of the model is still safe as it bears a safety factor above 1. Moreover, the displacement analysis as seen in Figure 5 shows that the force applied exerts negligible displacement since the greatest displacement experienced within the subassembly is 0.009371 mm. This would indicate that the model could handle slightly higher forces above 400 N.

3.3. Analysis of Sample Tool Subassembly

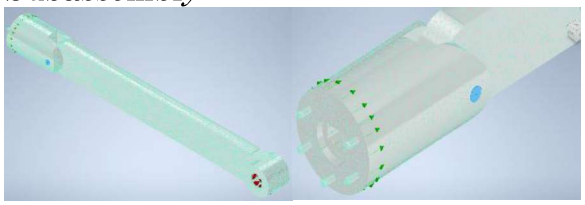

Fig 6. Specified constraints, loads, connections, and generated mesh for sample tool subassembly

The sample tool subassembly consists of three parts: (a) the rear, (b) the pin, and (c) the terminal device. The rear is the part of the tool that bears the locking mechanism which connects to the shaft extension. This is where the force is exerted as shown by the green arrows in Figure 6. It has a hole at the center where the shaft inserts and several protruding structures that connect with the holes on the motor casing. This improves the contact and load distribution between the surfaces of the subassemblies. The terminal device bears the actual tool that encloses the lug nut. The hole at the end acts as the constraint (as marked by the red arrows in Figure 6) since the lug nut is stiff prior to removing it. The two aforementioned parts are connected by a pin, which is highlighted in blue as seen in Figure 6.

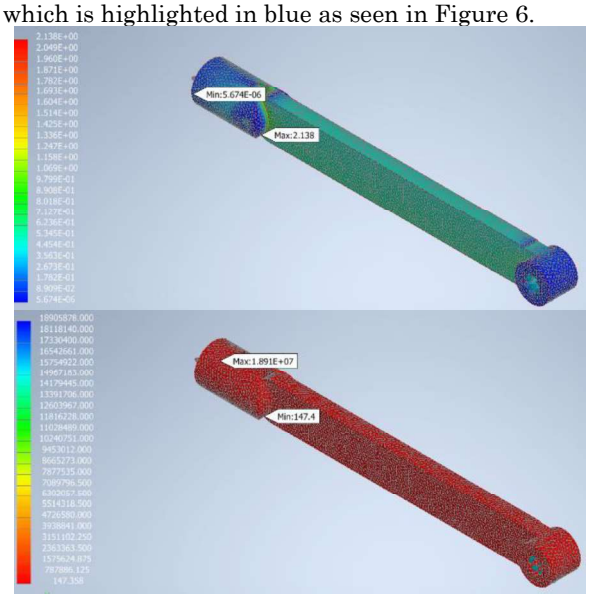

Fig 7. von Mises stress analysis (left), and safety factor analysis (right) of sample tool subassembly

All components of the sample tool are made of steel, which indicates that their Young's modulus, Poisson's ratio, and yield strength are 21000, 0.3, and 207 MPa respectively, similar to the specifications of the material properties in the previous subassembly.

As seen in Figure 7, the maximum stress experienced by the model is 2.138 MPa, which is significantly lower than the material's yield strength. This indicated that greater pushing forces could be exerted before the subassembly breaks. However, the concentrated area of relatively high stress at the pin indicates that further distribution of load if significantly greater forces will be applied. Though that is a reasonable observation, the minimum safety factor, which is 147.4, is also located at the pin. This shows that the model, especially the pin, can handle larger forces above 400 N since the minimum value is far beyond 1.

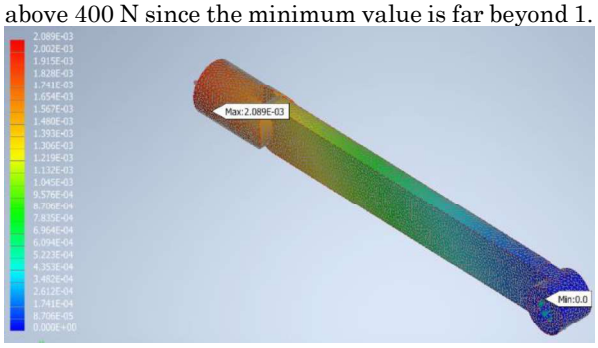

Fig 8. Displacement analysis of sample tool subassembly

The minuscule displacements presented in Figure 8 indicate that the subassembly is barely affected by the applied pushing force despite the long and slender terminal end. Though all indicators imply that the tool can handle the stress, the different angles the tool may be oriented would portray different results, which may affect the stress and displacement values of the device. Moreover, different directions of load application would also lead to varying displacement results. These situations, however, are no longer within the scope of the study but may be used for future studies.

4. CONCLUSIONS

The arm prosthesis design made for auto-mechanics is feasible since it can withstand one of the common forces exerted in car maintenance, namely the tightening and loosening of lug nuts. The individual subassemblies prove that their respective geometries and materials are able to withstand the applied force without significant displacements and yielding. Additionally, the ability of the exterior shell made of ABS to sustain the exerted force implies that it can be used as an alternative when creating arm prostheses. For further study, it is recommended to optimize the geometry of the components to disperse the load over a greater area. Additionally, different load orientations and tool orientations would be recommended to fully characterize the deformations and stress contours of the created prosthetic.

5. ACKNOWLEDGMENTS

We would like to thank our adviser Engr. Michael Manguerra for his continuous support and optimism throughout our work with this study. Even though the pandemic worsened conditions for almost everyone, he was still able to advise us properly and even help us gather our materials within the campus.

6. REFERENCES

Abd Rahman, N. I., Md Dawal, S. Z., Yusoff, N., & Mohd Kamil, N. S. (2018). Anthropometric measurements among four Asian countries in designing sitting and standing workstations. Sādhanā, 43(1). https://doi.org/10.1007/s12046-017-0768-8

Mina, C. D. (2003). Philippine Institute for Development Studies. https://pidswebs.pids.gov.ph/ris/dps/pidsdps1313.pdf

Ovadia, S., & Askari, M. (2015). Upper Extremity Amputations and Prosthetics. Seminars in Plastic Surgery, 29(01), 055–061. https://doi.org/10.1055/s-0035-1544171

Philippine Statistics Authority. (2013, January). Psa.gov.ph. https://psa.gov.ph/content/persons-disability-philippines-results-2010-census

Maduri, P., & Akhondi, H. (2019, May 18). Upper Limb Amputation. Nih.gov; StatPearls Publishing. https://www.ncbi.nlm.nih.gov/books/NBK540962/

Strait, E. (2006). Prosthetics in Developing Countries. ResearchGate; unknown. https://www.researchgate.net/publication/238088826_Prosthetics_in_Developing_Countries

Tirerack. (2021). Wheel Lug Torquing. https://www.tirerack.com/tires/tiretech/techpage.jsp?techid=107&fbclid=IwAR1bFk5NKSWeVU7s3233G_KFhNiA3IXoacb7WxKvDiN_BdqG-cAskt_Cnkohttps://www.tirerack.com/tires/tiretech/techpage.jsp?techid=107&fbclid=IwAR1bFk5NKSWeVU7s3233G_KFhNiA3IXoacb7WxKvDiN_BdqG-cAskt_Cnko

Vigotsky, A. D., Halperin, I., Lehman, G. J., Trajano, G. S., & Vieira, T. M. (2018). Interpreting Signal Amplitudes in Surface Electromyography Studies in Sport and Rehabilitation Sciences. Frontiers in Physiology, 8. https://doi.org/10.3389/fphys.2017.00985